ELSEVIER

Diamond and Related Materials 9 (2000) 765–770

DIAMOND AND RELATED MATERIALS

www.elsevier.com/locate/diamond

Defect and disorder reduction by annealing in hydrogenated tetrahedral amorphous carbon

N.M.J. Conway [a,*], A.C. Ferrari [a], A.J. Flewitt [a], J. Robertson [a], W.I. Milne [a], A. Tagliaferro [b], W. Beyer [c]

[a] *Department of Engineering, University of Cambridge, Cambridge CB2 1PZ, UK*
[b] *Dipartimento di Fisica, Politecnico di Torino, Torino 10129, Italy*
[c] *ISI-PV, Forschungszentrum Jülich, Jülich D52425, Germany*

Abstract

Hydrogenated tetrahedral amorphous carbon (ta-C:H) is a form of diamond-like carbon with a high sp^3 content (>60%), grown here using a plasma beam source. Information on the behaviour of hydrogen upon annealing is obtained from effusion measurements, which show that hydrogen does not effuse significantly at temperatures less than 500°C in films grown using methane and 700°C in films grown using acetylene. Raman measurements show no significant structural changes at temperatures up to 300°C. At higher temperatures, corresponding to the onset of effusion, the Raman spectra show a clustering of the sp^2 phase. The density of states of ta-C:H is directly measured using scanning tunnelling spectroscopy. The measured gradients of the conduction and valence band tails increase up to 300°C, confirming the occurrence of band tail sharpening. Examination of the photoluminescence background in the Raman spectra shows an increase in photoluminescence intensity with decreasing defect density, providing evidence that paramagnetic defects are the dominant non-radiative recombination centres in ta-C:H.

Keywords: Defects; Disorder; Effusion; Hydrogenation; Tetrahedral amorphous carbon

1. Introduction

Diamond-like carbon possesses a high paramagnetic defect density of the order of 10^{19} to $10^{20}\,cm^{-3}$ [1–4]. This is the case even in the hydrogenated forms, unlike in amorphous silicon where the addition of hydrogen can result in a four order of magnitude decrease in the defect density [5]. The presence of such a high defect density clearly has detrimental effects on the electronic potential of the material, as has been illustrated by its poor performance as the active layer in thin film transistors [6,7] and its small photoconductivity [8].

The defect density of PECVD a-Si:H is also improved considerably by deposition at elevated temperatures of around 300°C. Increasing the deposition temperature in DLC however leads to a more sp^2 bonded network [9,10]. Recent studies of post-deposition annealing to decrease the intrinsic compressive stress of ta-C films showed that, after deposition, films are stable to much higher temperatures [11] and therefore material improvement using elevated temperatures may be possible post-deposition. Our previous work using ta-C:H has shown this to be the case, with a factor of 25 decrease in the defect density after post-deposition annealing at 300°C and a simultaneous decrease in disorder, as evidenced by the decrease in the Urbach slope [12]. These effects have been attributed to improved passivation of defects and a modification of more weakly bonded sp^2 clusters with narrower local band gaps by migration of hydrogen through the C—C network. The sharpening of the band tails, as suggested by the decrease in the Urbach slope, was further confirmed by measurements of conductivity and activation energy. The defect density decrease was supported by photoconductivity measurements, which showed an increase in photosensitivity with annealing up to 300°C.

The work presented here expands on this initial study. As the effects observed upon annealing were attributed to the migration of hydrogen, it is useful to further

* Corresponding author. Present address: Lab. PICM, Ecole Polytechnique, 91128 Palaiseau-Cedex, France. Tel.: +33-69-333-683; fax: +33-69-33-3-006.
E-mail address: conway@poly.polytechnique.fr (N. Conway)

0925-9635/00/$ - see front matter
PII: S0925-9635(99)00271-X

understand the behaviour of hydrogen during the annealing process. To achieve this, mass-selected thermal effusion measurements are performed. The structure of the films under post-deposition annealing is also studied by examining the variation in Raman spectra upon annealing. Previous results, as summarised above, showed that there was a change in the conduction and valence band edges upon annealing. Recent work by Arena et al. [13] has shown that the density of states in ta-C could be examined directly using scanning tunnelling spectroscopy (STS). STS is therefore used here to examine the variation in the density of states (DOS) upon annealing in ta-C:H. Raman spectroscopy is also used to examine the variation in photoluminescence (PL) upon annealing.

2. Experimental details

The ta-C:H films were grown using a plasma beam source (PBS) [14,15]. In the PBS, the majority of ions exit the plasma with a similar ion energy, as defined by the plasma d.c. self-bias. This contrasts with the case of conventional PECVD, where the ions have a wide range of energy [16]. This improved control of the ion energy means that all ions can be tuned, by varying the r.f. power, to an optimum ion energy to promote sp^3 bonding, in a similar manner to the filtered cathodic vacuum arc for ta-C [17].

ta-C:H was grown using both methane [ta-C:H(meth)] and acetylene [ta-C:H(acet)] at a pressure of 10^{-4} mbar, flow rates of 2.5 and 5 sccm, and average ion energies of 130 and 200 eV (corresponding to $\sim$100 eV per carbon ion), respectively. Both types of film have been extensively characterised. The sp^2 contents measured by EELS are similar in both cases, at $\sim$35%. The density of the acetylene based films is greater, however, as it contains only 30% hydrogen relative to 43% in the methane films. Additionally, there is 4 at% nitrogen present in the ta-C:H(acet) films due to impurities in the acetylene gas, making it slightly n-type [15]. The ta-C:H(acet) films do, however, exhibit similar variations upon annealing to those described in the introduction for ta-C:H(meth) [18].

The STS measurements were performed using an Oxford Instruments, W.A. Technology Mark III ultra-high vacuum scanning tunnelling microscope, using the model described by Arena et al. [13]. ta-C:H:N(acet) samples were grown for STS on high doped n-type silicon substrates (0.02 Ω cm resistivity). STS could not be performed on ta-C:H(meth) films due to their high resistivity. For each set of STS measurements, successive anneals were performed on the same sample without breaking vacuum. Unpolarised Raman spectra were recorded in backscattering geometry for 514.4 nm excitation from an Ar ion laser using a Jobin-Yvon T64000 triple grating spectrometer. The samples for Raman measurements were grown on low doped silicon substrates and were annealed under vacuum between 100 and 1000°C at 100°C intervals. For the effusion measurements, samples deposited on low doped silicon were heated up to 1050°C at a rate of 20°C/min. The effusing species were pumped through a quadrupole mass analyser (QMA) which simultaneously recorded the partial pressure of the 14 different masses corresponding to the most prominent hydrocarbon effusing species. Helium flow was also measured through a calibrated capillary to ensure the stability of the QMA. Samples for electron-spin resonance and photodeflection spectroscopy (PDS) were grown on 7059 Corning glass substrates and annealed in a nitrogen atmosphere. All anneals were 15 min in duration.

3. Results and discussion

Fig. 1a shows the mass-selected thermal effusion characteristics of ta-C:H(meth). The dominant effusion species is H_2, although there is also significant effusion of H, CH_4, C_2H_4 and CH_3 species. The majority of species do not effuse until temperatures of $\sim$500°C and peak at 600°C, however, there is a small peak of H_2 around 200°C. This may be due to a small amount of hydrogen trapped in voids within the film.

The thermal effusion characteristics of ta-C:H(acet) are shown in Fig. 1b. Again, the dominant effusion species are hydrogen, but there is a much smaller amount of effusion of hydrocarbon species than in ta-C:H(meth). The majority of hydrogen in this case does not effuse until higher temperatures of around 700°C. No peak in the H_2 effusion line is observed at low temperatures in this case. These characteristics point to a more dense structure in ta-C:H(acet) than ta-C:H(meth), as reflected in their microscopic densities obtained from EELS measurements. The characteristics of ta-C:H(acet) are similar to those found by Stief et al. [19] for acetylene-grown ta-C:H. The ta-C:H(meth) is similar to that observed for the optimum PECVD-deposited hard a-C:H. The increase in the amount of effusion of hydrocarbon species in the case of ta-C:H(meth) implies a reduced amount of cross-linking within the structure. In both cases, however, the majority of effusion occurs at temperatures much higher than 300°C, and hence at greater temperatures than the defect density reduction.

Fig. 2a and b shows the Raman spectra for as-deposited ta-C:H(acet) and ta-C:H(meth), respectively. The spectra consist of a main band due to the relative motion of sp^2 carbon atoms (G peak) at 1537 cm^{-1} [ta-C:H(acet)] and 1522 cm^{-1} [ta-C:H (meth)], and of a low frequency modulation corresponding to ring-breaking modes (D peak) at $\sim$1280 cm^{-1},

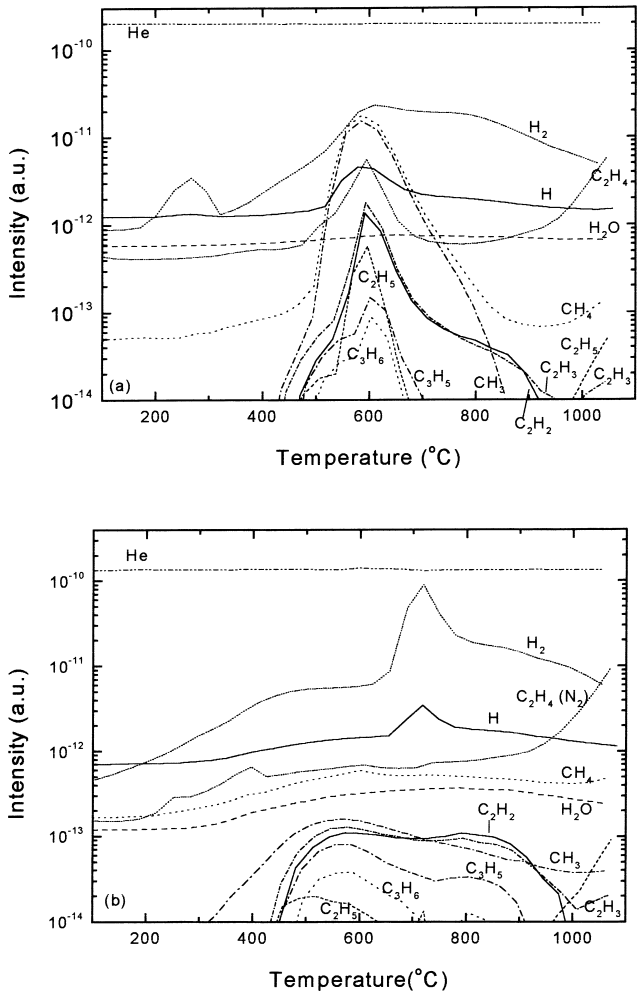

Fig. 1. Mass-selected thermal effusion characteristics of (a) ta-C:H(meth) and (b) ta-C:H(acet).

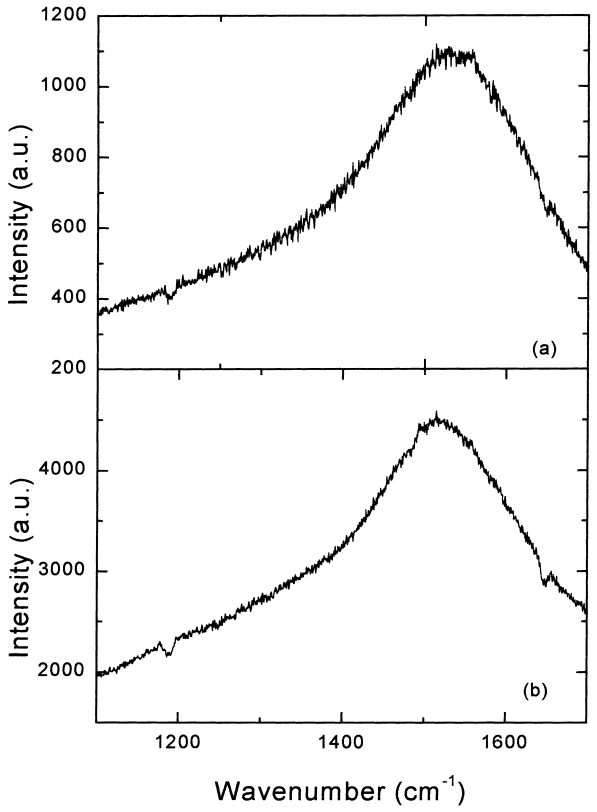

Fig. 2. Raman spectra of as-deposited (a) ta-C:H(acet) and (b) ta-C:H(meth).

which contrasts with ta-C, where no D peak is visible [20]. Good fits to all the spectra through the annealing process were obtained using a combination of Breit–Wigner–Fano (BWF) for the G peak and Lorentzian for the D peak [20], and a linear background to account for the photoluminescence. The maximum of the BWF is used to define the G peak position. The as-deposited ta-C:H(acet) sample has a higher G position and a lower $I(D)/I(G)$ than the corresponding ta-C:H(meth) sample. This implies a lower clustering of the sp^2 phase for the ta-C:H(acet).

Fig. 3a and b shows the variation with annealing temperature of the G peak position and the ratio of the Raman scattering intensity of the D and G peaks, $I(D)/I(G)$, respectively. It can be seen that both the G peak position and $I(D)/I(G)$ increase sharply above 400°C in ta-C:H(meth) and 600°C in ta-C:H(acet). The increase in the G position towards that of graphite suggests an increase in amount of sp^2 bonding and ordering within the sp^2 phase. The increase in $I(D)/I(G)$ means that there is an increase in the number of ordered aromatic rings within the sample. There is, however, little observed change in structure from the Raman data up to temperatures of 300°C, where the defect reduction has been shown to occur [12], with a possible small decrease in the G peak position and $I(D)/I(G)$ up to ~200°C.

Comparison with the effusion data in Fig. 1 shows that the change in structure observed in the Raman spectra in both cases occurs at a similar temperature to where there is significant effusion from the films. This suggests that at temperatures of around 400°C in ta-C:H(meth) and 600°C in ta-C:H(acet), bonded hydrogen begins to effuse from the films and the film subsequently reorders itself into a more graphitic structure. A similar decrease in sp^3 fraction with hydrogen effusion has also been observed in a-C:H [21].

Fig. 4a shows the variation in the DOS profile obtained for ta-C:H(acet) using STS upon annealing up to temperatures of 650°C. The tip to sample separation for each STS measurement is determined by setting a current of 50 pA at +2 V, and therefore the tip height need not be the same in each measurement, and only the relative shape of the spectra and not the magnitude of the DOS can be compared. This is why the closure of the gap at higher annealing temperatures cannot be observed by this method.

In order to examine the variation in shape of the

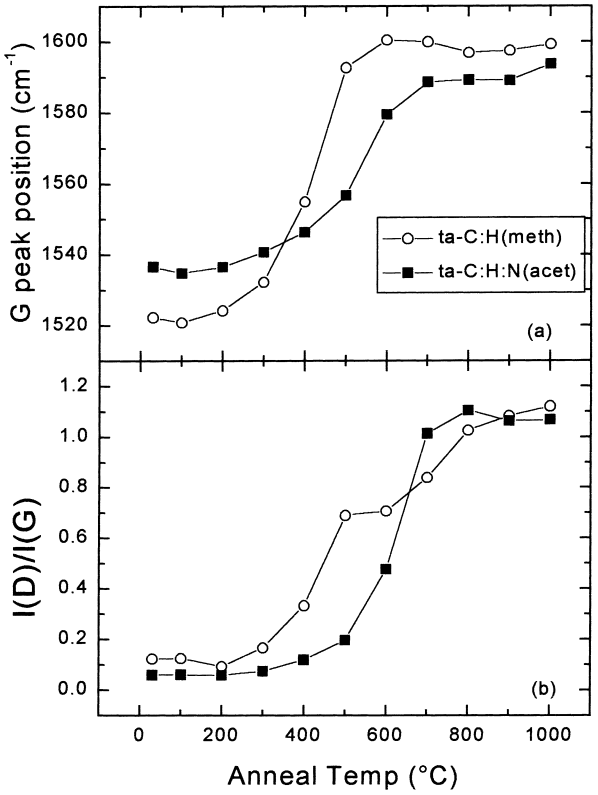

Fig. 3. Variation in (a) G peak position and (b) $I(D)/I(G)$ ratio with annealing for ta-C:H(meth) and ta-C:H(acet).

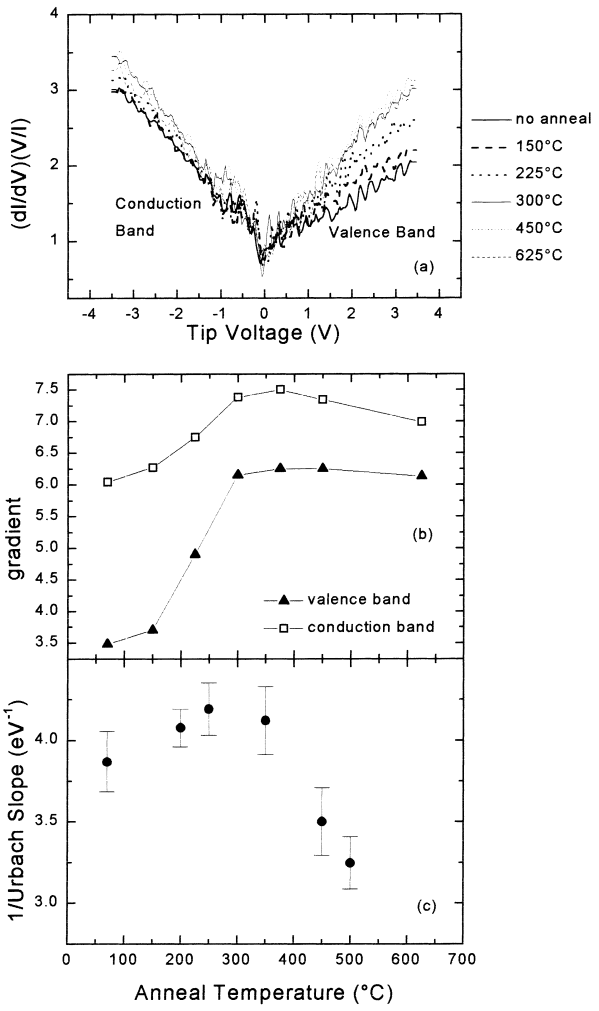

Fig. 4. Variation in (a) DOS profile for ta-C:H(acet) measured by STS, (b) the conduction and valence band gradients and (c) $1/E_0$ as measured by PDS with annealing.

conduction and valence bands, their gradients at each annealing temperature were taken over the regions -1 to -3 V and $+1$ to $+3$ V, respectively and are shown in Fig. 4b. The valence band shows an increase in gradient with annealing up to temperatures of 300°C, after which it remains relatively constant. The gradient of the conduction band edge does not vary as greatly, but also shows an increase in gradient up to 300°C. In other words, examination of the density of states by STS shows a sharpening of the conduction and valence bands over the examined energy range upon annealing up to 300°C, after which there is little further change in overall shape. The variation of the Urbach slope, E_0, was obtained from PDS measurements as described previously [12]. $1/E_0$ is proportional to the slope of the band tails in the energy range just below the E_{04} gap [5] and its variation with annealing temperature is shown in Fig. 4c. These results also show an increase in gradient up to 300°C and hence imply a sharpening of the band tails. At higher temperatures, $1/E_0$ decreases sharply, which contrasts with the behaviour of the slope shown in Fig. 4b. However, STS examines the slopes over a constant energy range, whereas the Urbach slope was measured over the same absorption range. Thus at higher temperatures where the optical gap decreases, E_0 is measured at lower energies and no longer over a similar energy range to the STS measurements.

Marchon et al. [22] proposed the ratio between the PL background slope and the G peak intensity of the Raman spectra, $m/I(G)$, as a convenient way to estimate the PL intensity in a-C:H. Fig. 5a shows the variation in PL intensity for ta-C:H(acet) and ta-C:H(meth), where the relative intensity of ta-C:H(acet) is 10 times less than that of ta-C:H(meth). The variation in defect density for ta-C:H(meth) as measured by electron spin resonance and the variation in optical band gap is shown in Fig. 5b. It can be seen that the PL increases as the defect density decreases up to a temperature of 300°C. The mechanism for PL in a-C:H is still a matter of debate. In a-Si:H, it is well known that the paramagnetic defects act as the dominant non-radiative recombination centres, however, a number of authors have demonstrated a poor correlation between paramagnetic defect density and PL efficiency in a-C:H [2,23]. Giorgis et al. suggested that one also had to take into account mid-gap defects that could not be measured by ESR [24]. Robertson [25] demonstrated that it is possible to fit a

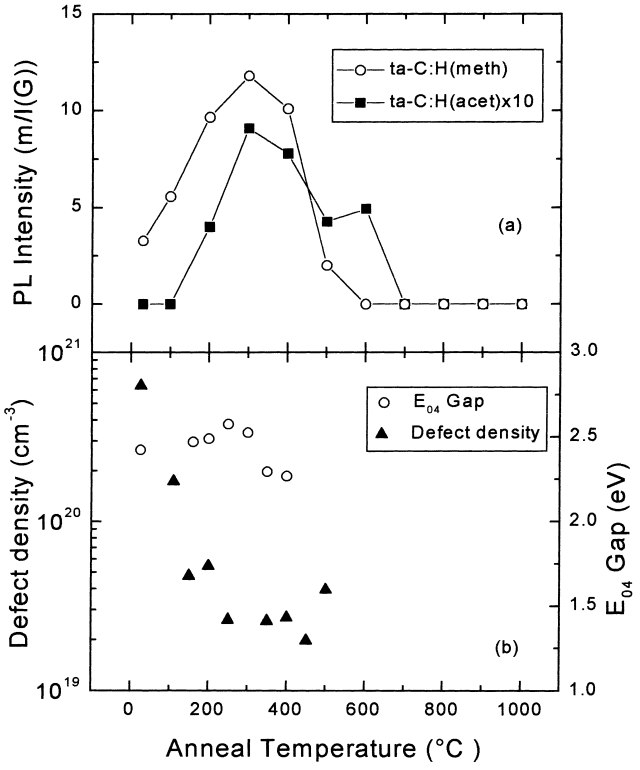

Fig. 5. Variation in (a) PL intensity and (b) paramagnetic defect density and optical gap with annealing.

model similar to the Street model for a-Si:H [5] to the lower band gap forms of a-C:H, taking the ESR-measured paramagnetic defects as the dominant non-radiative recombination centres, if one assumes a much smaller capture radius of 20 Å. It was also suggested that the majority of the problems with fitting the Street model to the PL data may arise due to a variation in localisation radius, and hence capture radius with band gap [4]. In the case presented here, there is a decrease in the defect density with relatively little variation in the optical band gap and hence capture radius. The fact that the PL efficiency increases as the defect density decreases provides evidence to suggest that paramagnetic defects do act as the main recombination centres in ta-C:H. Additionally, the annealing temperature at which the PL is quenched in both materials corresponds to the energy at which there is effusion of hydrogen and hence graphitisation of the film as described above. This can be related to the increase in states further into the gap width, and hence creation of electron–hole pairs closer to the non-radiative mid-gap defects.

These results show that the effect of annealing on ta-C:H can be divided into two separate stages. At low annealing temperatures up to ~300°C, there is modification of the band structure and a reduction in defect density caused by hydrogen migration, whilst no significant effusion of hydrogen from the films or major changes in structure are observed. At higher temperatures, the annealing causes the effusion of hydrogen and a subsequent re-ordering to a more graphitic structure. The onset of this stage is determined by the density of the film, with a denser, more cross-linked, film remaining stable to higher temperatures.

4. Conclusions

This paper has studied the effects of post-deposition annealing on ta-C:H. At temperatures less than 300°C, short-range migration of hydrogen within ta-C:H as well as network reconstruction results in defect passivation, as seen by the decrease in paramagnetic defect density. Hydrogen effusion measurements demonstrate that there is little effusion of hydrogen up to ~500°C in ta-C:H(meth) and ~700°C in ta-C:H(acet). Raman measurements also show no structural changes at low temperatures, but an increase in graphitisation at similar temperatures to the onset of hydrogen effusion. Direct examination of the density of states using STS confirms a sharpening of the band edges up to 300°C, as suggested by previous measurements [12], after which the overall shape of the DOS stays relatively constant. The PL background in the Raman spectra shows that the PL intensity increases with decreasing defect density in both cases, which suggests that the non-radiative recombination centres in ta-C:H are paramagnetic defects.

Acknowledgements

The authors thank Professor C.E. Bottani of Politecnico di Milano for the Raman facilities. N.M.J. Conway acknowledges the financial support of the EPSRC and Philips Research Laboratories, Redhill, UK. A.C. Ferrari acknowledges funding by a European Community TMR Marie Curie Fellowship.

References

[1] M. Hoinkis, E.D. Tober, R.L. White, M.S. Crowder, Appl. Phys. Lett. 61 (1992) 2653.
[2] S. Schutte, S. Will, H. Mell, W. Fuhs, Diamond Relat. Mater. 2 (1993) 1360.
[3] J. Ristein, J. Schafer, L. Ley, Diamond Relat. Mater. 4 (1995) 508.
[4] Rusli, J. Robertson, G.A.J. Amaratunga, J. Appl. Phys. 80 (1996) 2998.
[5] R.A. Street, Hydrogenated Amorphous Silicon, Cambridge University Press, Cambridge, 1991.
[6] F.J. Clough, W.I. Milne, B. Kleinsorge, J. Robertson, G.A.J. Amaratunga, B.N. Roy, Electron. Lett. 32 (1996) 319.
[7] S. Maeng, S. Uchikoga, F. Clough, A. Tagliaferro, J. Robertson, W.I. Milne, Diamond Relat. Mater. (1999) this issue.

[8] A. Ilie, N.M.J. Conway, B. Kleinsorge, J. Robertson, W.I. Milne, J. Appl. Phys. 84 (1998) 5575.
[9] F.W. Smith, J. Appl. Phys. 55 (1984) 764.
[10] S. Sattel, J. Robertson, H. Ehrhardt, J. Appl. Phys. 82 (1997) 4566.
[11] T.A. Friedmann, J.P. Sullivan, J.A. Knapp, D.R. Tallant, D.M. Follstaedt, D.L. Medlin, P.B. Mirkarimi, Appl. Phys. Lett. 71 (1997) 3820; A.C. Ferrari, B. Kleinsorge, N.A. Morrison, A. Hart, V. Stolojan, J. Robertson, J. Appl. Phys., 85 (1999) 7191.
[12] N.M.J. Conway, A. Ilie, J. Robertson, W.I. Milne, A. Tagliaferro, Appl. Phys. Lett. 73 (1998) 2456.
[13] C. Arena, B. Kleinsorge, J. Robertson, W.I. Milne, M.E. Welland, J. Appl. Phys. 85 (3) (1999) 1609.
[14] M. Weiler, S. Sattel, T. Giessen, K. Jung, H. Ehrhardt, V.S. Veerasamy, J. Robertson, Phys. Rev. B 53 (1996) 1594.
[15] N.M.J. Conway, W.I. Milne, J. Robertson, Diamond Relat. Mater. 7 (1997) 477.
[16] C. Wild, P. Koidl, Appl. Phys. Lett. 51 (1987) 1506.
[17] M. Chhowalla, C.A. Davies, M. Weiler, B. Kleinsorge, G.A.J. Amaratunga, J. Appl. Phys. 79 (1996) 2237.
[18] N.M.J. Conway, Ph.D. Thesis, Cambridge University, 1998.
[19] R. Stief, J. Schafer, J. Ristein, L. Ley, W. Beyer, J. Non-Cryst. Solids 198 (1996) 636.
[20] S. Prawer, K.W. Nugent, Y. Lifshitz, G.D. Lempert, E. Grossman, J. Kulik, I. Avigal, R. Kalish, Diamond Relat. Mater. 5 (1996) 433.
[21] D.R. Tallant, J.E. Parmeter, M.P. Siegal, R.L. Simpson, Diamond Relat. Mater. 4 (1995) 191.
[22] B. Marchon, J. Gui, K. Grannen, G.C. Rauch, J.W. Ager III,, S.R.P. Silva, J. Robertson, IEEE Trans. Magn. 27 (1991) 5160.
[23] S. Liedtke, K. Lips, K. Jahn, W. Fuhs, J. Non-Cryst. Solids 114 (1989) 522.
[24] F. Giorgis, F. Giuliani, C.F. Pirri, A. Tagliaferro, E. Tresso, Appl. Phys. Lett. 72 (1998) 2520.
[25] J. Robertson, Philos. Mag. B 76 (3) (1997) 335.